Dynamic and Static Approaches to Quantifying ^{18}F-FDG Uptake for Measuring Cancer Response to Therapy, Including the Effect of Granulocyte CSF

Robert K. Doot[1,2], Lisa K. Dunnwald[2], Erin K. Schubert[2], Mark Muzi[2], Lanell M. Peterson[2], Paul E. Kinahan[1,2], Brenda F. Kurland[3], and David A. Mankoff[1,2]

[1]Department of Bioengineering, University of Washington, Seattle, Washington; [2]Division of Nuclear Medicine, University of Washington, Seattle, Washington; and [3]Clinical Research Division, Fred Hutchinson Cancer Research Center, Seattle, Washington

The response of cancer to chemotherapy can be quantified using ^{18}F-FDG to indicate changes in tumor metabolism. Quantification using the standardized uptake value (SUV) is more feasible for clinical practice than is the metabolic rate of ^{18}F-FDG (MRFDG), which requires longer, dynamic scanning. The relationship between MRFDG and SUV depends in part on how each accounts for blood clearance of tracer. We tested whether chemotherapy and treatment with granulocyte colony-stimulating factor (CSF) changed the blood clearance curves and therefore affected the relationship between MRFDG and SUV. **Methods:** Thirty-nine patients with locally advanced breast cancer underwent ^{18}F-FDG PET before and after chemotherapy, including granulocyte CSF. The area under the curve (AUC) for blood clearance was determined before and after therapy. MRFDGs were determined by graphical analyses, whereas SUVs were calculated using the standard formula normalized by body weight. MRFDG and SUVs were compared with each other and with tumor response. Paired percentage changes in MRFDG and SUV were also divided into tertiles based on pretherapy SUV to investigate differences in the relative sensitivity of SUV changes to MRFDG changes due to baseline tumor uptake. **Results:** Despite a small but statistically significant 6% decrease in blood AUCs after therapy ($P = 0.02$), SUV and MRFDG did not differ significantly in slope ($P = 0.53$) or in correlation before and after therapy ($r = 0.95$ for both). Percentage changes in MRFDG and SUV between serial scans correlated with each other ($r = 0.84$) and with patient response ($P \leq 0.06$). The maximum detectable percentage change in SUV and the slope of percentage changes in MRFDG versus SUV for the patient tertile with the lowest baseline SUVs (65% $\pm$ 5% [$\pm$SE], slope (m) = 0.40 $\pm$ 0.12, n = 13) were significantly lower than for the other patients (86% $\pm$ 3%, m = 0.85 $\pm$ 0.10, n = 26, P = 0.01 for both). **Conclusion:** Chemotherapy and granulocyte CSF treatment resulted in a lower ^{18}F-FDG blood AUC. The maximum detectable percentage change in ^{18}F-FDG uptake is less when quantifying via static SUV than via dynamic MRFDG. This effect is small in most patients but may have clinical significance for measuring the response of patients with a low pretherapy ^{18}F-FDG uptake.

Key Words: SUV; MRFDG; ^{18}F-FDG; granulocyte CSF; response to therapy

The response of a tumor to therapy can be quantified by measuring changes in tumor glucose metabolism via serial PET scans of the glucose analog ^{18}F-FDG (*1–3*). Clinicians most frequently quantify tumor glucose metabolism from static images using the standardized uptake value (SUV) despite known limitations (*4–6*), including the inability to separate background from tumor activity. Tumor metabolism can also be quantified from dynamic scans using a 2-compartment model (*7,8*) that allows calculation of the metabolic rate of ^{18}F-FDG (MRFDG) from the tumor ^{18}F-FDG flux constant, K_i, estimated via either nonlinear regression or graphical analysis (*9,10*). The merits of full kinetic analysis of dynamic scans versus static imaging have been extensively discussed in the literature (*2,4–6,11–13*).

Neoadjuvant treatment of locally advanced breast cancer at our institution often includes granulocyte colony-stimulating factor (CSF), a hematopoietic cytokine that helps support adequate concentrations of neutrophils and in the process alters the biodistribution of ^{18}F-FDG (*14,15*). Granulocyte CSF therapy has been reported to significantly reduce blood levels of ^{18}F-FDG in rats (*15*). The effect of granulocyte CSF on ^{18}F-FDG uptake values has been reported for 18 patients with either primary locally advanced breast cancer or breast cancer metastasized to the lymph nodes, liver, lung, or bone. The study reported a high correlation between MRFDG, lean body mass, and glucose-normalized

SUV before therapy and a significant decrease from a baseline *r* value of 0.96 to 0.84 after 3 cycles of chemotherapy (63 d) that included either granulocyte CSF or granulocyte–macrophage CSF (*16*).

The goal of our analysis was to use a larger, more uniform patient population to determine the impact of applying either dynamic or static ^{18}F-FDG scans to quantify the response to chemotherapy regimes that could alter the biodistribution of PET tracers. Our hypothesis was that a change in tracer biodistribution between serial scans caused by factors such as granulocyte CSF may affect the relationship between MRFDGs and SUVs, because only quantification of the dynamic images (MRFDG) can directly compensate for the change in tracer dose available to the tumor. To this end, we studied the impact of granulocyte CSF–containing chemotherapy on the amount of tracer available to tumors and the linear relationship between MRFDG and SUV before and after therapy, and we examined the relationships between the percentage changes in MRFDG and SUVs and patient response.

MATERIALS AND METHODS

Patient Characteristics

We retrospectively analyzed 39 patients with ductal locally advanced breast cancer who underwent serial ^{18}F-FDG PET before and after approximately 10 wk of neoadjuvant chemotherapy that included granulocyte CSF (filgrastim [Neupogen]; Amgen). The patients were participants in an ongoing prospective study whose selection criteria, treatment, and response assessment were previously described (*17–19*). Most patients (*n* = 37) received dose-dense weekly anthracycline (doxorubicin), with 35 also receiving daily cyclophosphamide and 2 receiving both cyclophosphamide and fluorouracil. The 2 remaining patients underwent weekly taxane-containing regimens. The typical granulocyte CSF dose of 5 μg/kg/d was administered every day except on the day of weekly intravenous chemotherapy. The granulocyte CSF dose was reduced by 25%–50% if the patient experienced bone pain and had a neutrophil count above 20,000/mL (*20*).

Tumor response was assessed through surgical pathologic examination of posttherapy tumors excised via lumpectomy or mastectomy. A complete response required absence of macroscopic tumor by histopathologic examination. A partial response indicated a greater than 50% reduction in residual tumor from baseline mass as measured via ultrasound, mammography, or physical examination. All other tumor responses were recorded as no response. The patients provided signed informed consent for the PET studies according to the guidelines of the University of Washington Human Subjects Committee.

PET

Our PET acquisition parameters and ^{18}F-FDG production methods were previously described (*17–19*), and a brief summary follows. Patients were scanned using an Advance tomograph (GE Healthcare) for 60 min after infusion of 216–391 MBq of ^{18}F-FDG. Regions of interest (ROIs) consisting of 1.5-cm-diameter circles were drawn over the breast tumor and the left ventricle of the heart to determine the tumor and blood time–activity curves. The same tumor ROI data were used for both the MRFDG and the SUV algorithms to avoid any comparison error due to the ROI placement (*11*).

Data Analysis

Areas under the curve (AUCs) for the blood time–activity curves from 0 to 60 min were calculated using trapezoidal integration to quantify the total amount of tracer available to tumors. The resulting AUCs in units of (Bq/mL) × min were converted into (SUV units) × min for individual patient scans.

Standard Patlak-Gjedde graphical analysis (*10*) was used to estimate the tracer flux constant, K_i (mL/min/g), using the tumor and blood time–activity curves from 30 to 60 min after injection. The MRFDG value (μmol/min/100 g) was calculated by multiplying K_i by the patient plasma glucose concentration (μmol/mL). The resulting MRFDG values served as the basis for interpreting ^{18}F-FDG tissue uptake, because the dynamic algorithm can account for changes in the available tracer due to chemotherapy and granulocyte CSF treatment (*11,21*).

SUV was calculated using the standard weight-based formula. We determined the static tumor uptake by averaging the 3 time bins taken from 45 to 60 min. We also calculated average SUVs from 30 to 60 min and using glucose, lean body mass, and body surface area formulas and found similar or lower correlation results when compared with MRFDG or K_i values.

Statistics

The difference between the AUC for the blood time–activity curves was examined using a 2-tailed, paired Student *t* test. Linear relationships between MRFDG and SUV were modeled using generalized estimating equations to account for correlations between serial measurements. To investigate the role of higher uncertainty in percentage change in MRFDG and SUV at lower initial values (*12,22*), additional regression models fitted separate intercepts (percentage change in SUV for a 100% reduction in MRFDG) and slopes for patient tertiles grouped by pretherapy SUV. Percentage changes in MRFDG and SUVs were related to patient response using Wilcoxon and Kruskal–Wallis tests. The areas of receiver-operating-characteristic curves for discrimination of no response from response using percentage changes in MRFDG and SUV were also compared nonparametrically (*23*). Statistical analyses were conducted using a combination of Excel spreadsheets (Microsoft); JMP 5.0 and SAS 9.1 (SAS Institute); and R, version 2.2.1 (R Foundation for Statistical Computing). *P* values less than 0.05 were considered significant.

RESULTS

Patient Characteristics

General patient characteristics have previously been reported (*17–19*) and are summarized below. Thirty-nine patients with ductal locally advanced breast cancer underwent serial ^{18}F-FDG PET before and after a mean of 72 d (±18 d, SD) of neoadjuvant chemotherapy that included granulocyte CSF. The mean patient age was 47 y, mean baseline tumor size was 5.5 cm (range, 1.1–11.0 cm), and clinical TN stage ranged from T1 N1 to T4 N2 disease, with 10% diagnosed with inflammatory T4 carcinomas. Seventeen of the patients had a complete macroscopic pathologic response, 17 had a partial response, and 5 had no response. Serial PET images of a patient who achieved a complete response are shown in Figure 1.
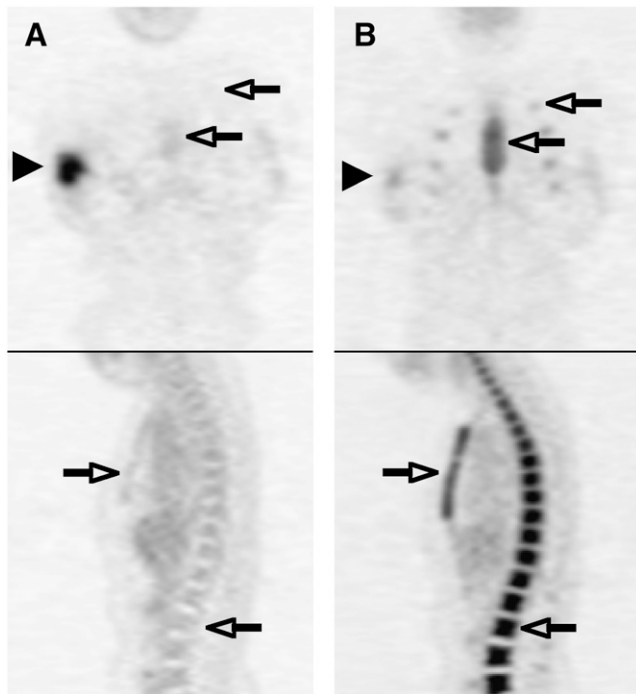
FIGURE 1. Coronal and sagittal ^{18}F-FDG PET images of same patient before treatment (A) and after neoadjuvant chemotherapy including granulocyte CSF (B). Right breast cancer decreased in ^{18}F-FDG activity after treatment (arrowheads), whereas ^{18}F-FDG activity increased in marrow in spine, sternum, and ribs (open arrows).

AUCs for Blood Time–Activity Curves

AUCs for blood time–activity curves were calculated to test our hypothesis that the total amount of tracer available to tumors would decrease after granulocyte CSF–containing chemotherapy. The mean blood clearance curves for the 39 patients before and after therapy are shown in Figure 2. The small 6% decrease in average blood AUCs after chemotherapy and granulocyte CSF treatment was statistically significant (10.7 ± 4.4 SUV units × min [±SE], $P = 0.02$).

MRFDG and SUV Relationship Before and After Therapy

SUVs were plotted versus MRFDGs before and after therapy in Figure 3 to assess any impacts that the reduced total amount of available tracer due to therapy had on their correlation. The pretreatment slope of 0.33 SUV units per MRFDG units did not differ ($P = 0.53$) from the posttreatment slope of 0.32 SUV units per MRFDG units. The pretreatment intercept of 1.22 significantly differed ($P = 0.04$) from the posttreatment intercept of 0.87. When linear regression models were fitted for pre- and posttherapy values separately, the correlation coefficient was 0.95 for each.

Relationships Between Percentage Changes in MRFDG and SUV

The linear relationship between percentage changes in MRFDG and in SUV after chemotherapy and granulocyte CSF treatment ($r = 0.84$, slope [m] = 0.75 ± 0.08, $n = 39$) is seen in Figure 4A. To investigate the impact of pretherapy ^{18}F-FDG uptake on response quantification, we also examined changes in SUV versus MRFDG grouped by baseline SUV (Fig. 4 and Table 1). The slope for the percentage changes in SUV versus MRFDG in the tertile of patients with the lowest baseline SUV (m = 0.40 ± 12, $n = 13$) was significantly different ($P = 0.01$) from the slope calculated with the other patients (m = 0.85 ± 0.10, $n = 26$).

The absolute value of the y-intercept at MRFDG = -100% for plots of percentage changes in SUV versus MRFDG estimates the absolute maximum detectable percentage change in SUV when glucose metabolism has been completely shut down. This estimation indicates the potential impact of the background of nonphosphorylated ^{18}F-FDG on the static SUV measurement of response for patient populations with different ranges of baseline SUVs. The 65% maximum detectable percentage change in SUV for the patient tertile with the lowest initial SUV (SUV$_{pre}$ ≤ 3.0, 65% ± 5%, $r = 0.71$, $n = 13$) in Figure 4B was significantly lower ($P = 0.01$) than the 86% maximum detectable percentage change in SUV for patients with higher pretherapy SUVs (SUV$_{pre}$ > 3.0, 86% ± 3%, $r = 0.89$, $n = 26$) in Figure 4C.

Percentage Changes in MRFDG and SUV Relationships with Patient Response

Nonparametric tests found the percentage changes in MRFDG and SUV to differ by response category. Percentage
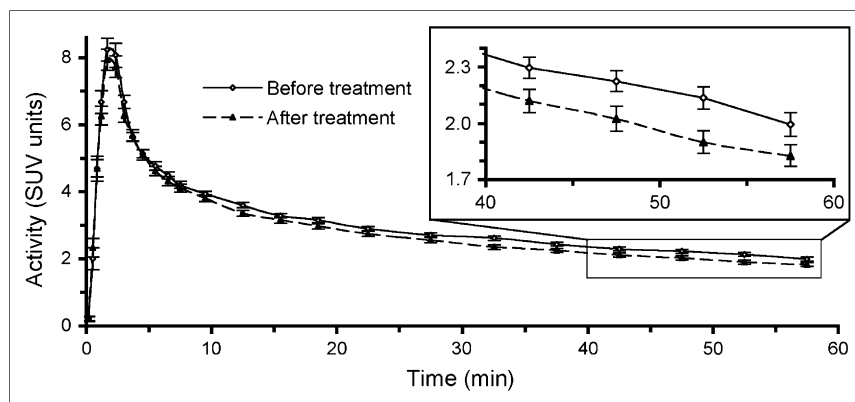

FIGURE 2. Mean ^{18}F-FDG blood clearance time–activity curves for patients ($n = 39$) before treatment and after chemotherapy including granulocyte CSF, with close-up of last 4 time bins with SE bars on middle time points (inset). Area under curve significantly decreased after treatment ($P = 0.02$).
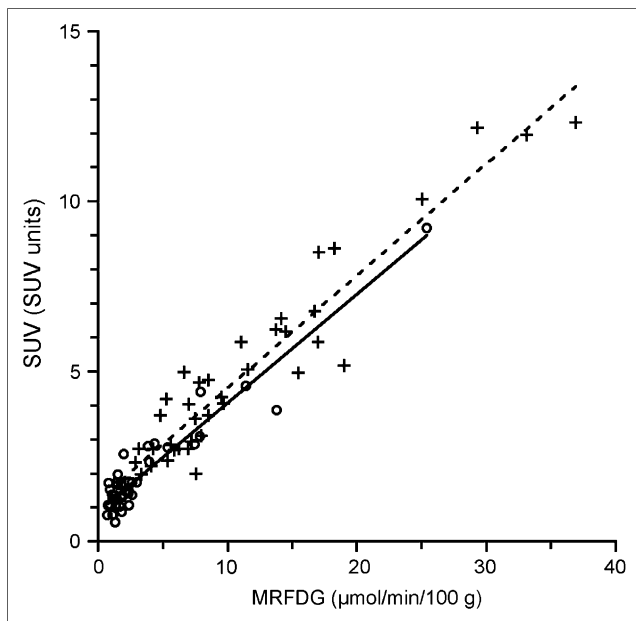
FIGURE 3. SUV vs. MRFDG for all patients before treatment (+ and dashed line) and after granulocyte CSF–containing chemotherapy regimes (○ and solid line).

changes in both MRFDG and SUV significantly correlated with pathology response and no response ($P = 0.005$ and 0.02, respectively). Percentage changes in MRFDG were related ($P = 0.02$) to no response, partial response, or complete response, whereas percentage changes in SUV demonstrated a trend toward association ($P = 0.06$) with 3 response categories. The areas under receiver-operating-characteristic curves for discrimination of no response from response using percentage changes in MRFDG and SUV (areas of 0.89 and 0.82, respectively) did not differ significantly ($P = 0.14$).

DISCUSSION

This study examined the relationship between MRFDG and SUV methods used to quantify tumor ^{18}F-FDG uptake and the relationship to patient response during therapy. We report a small but statistically significant decrease in the amount of ^{18}F-FDG tracer available to patient tumors after chemotherapy that includes granulocyte CSF treatment, as measured by the blood clearance AUC. This decrease is likely the result of the change in the biodistribution of ^{18}F-FDG tracer after therapy that is apparent in Figure 1 as increased uptake by the marrow. The 6% decrease in available tracer in our study was small and may not be clinically important; the SD of the mean percentage differences between blood AUCs was 8% in a previous ^{18}F-FDG PET test–retest study of 11 men and 5 women with metastatic cancer using ROIs drawn either in the left ventricular cavity ($n = 11$) or the aorta ($n = 5$) (12). However, our result is consistent with a previously reported trend ($P = 0.08$) toward lower blood ^{18}F-FDG activity in 16 breast cancer patients treated with chemotherapy regimes containing granulocyte CSF (15). The same report found that rats injected with granulocyte CSF had significantly lower blood levels of ^{18}F-FDG than rats injected with saline (15). This finding suggests that our observed decrease in blood ^{18}F-FDG uptake was due primarily to granulocyte CSF, though our study was not designed to separate the effects of individual chemotherapy components.

The comparable relationships between dynamic MRFDG and static SUVs found before and after therapy using 39 locally advanced breast cancer patients is consistent with previous studies that examined smaller, less uniform patient populations. Our findings of high correlations between MRFDG and SUV agree with prior studies performed on patients with gastroesophageal, breast, and non–small cell lung cancer (16,21,24)—studies that reported high correlations between values calculated for ^{18}F-FDG tumor uptake
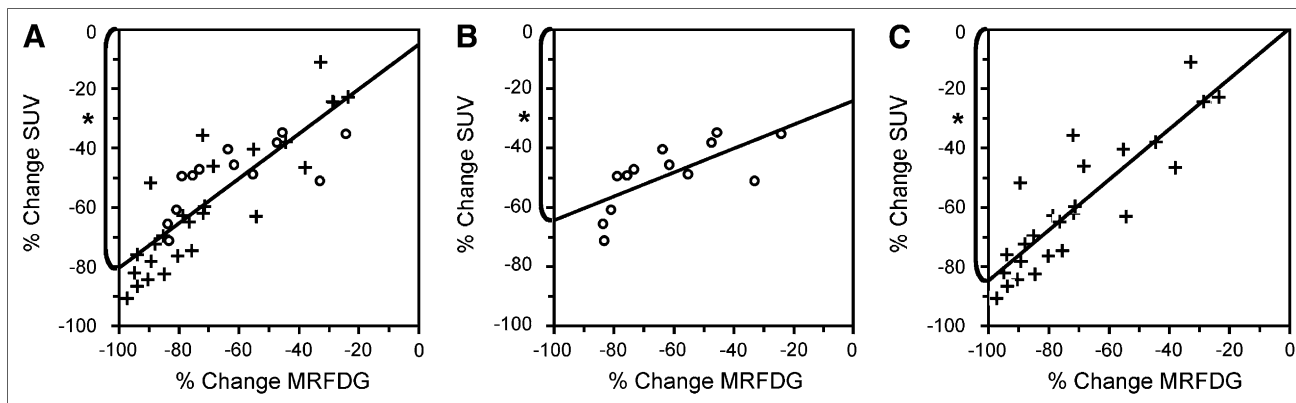

FIGURE 4. Percentage change in SUV vs. percentage change in MRFDG for all ($n = 39$) patients (A), first patient tertile (○, $n = 13$) with lowest baseline SUVs (B), and second and third patient tertiles (+, $n = 26$) with higher baseline SUVs (C). Maximum detectable percentage change in SUV (*) is mean percentage alteration in tumor metabolism that can be detected using SUV algorithm assuming that MRFDG model can detect 100% decrease in tumor metabolic activity.

TABLE 1
Linear Regression Parameters for Changes in SUVs Versus MRFDGs from Before to After Therapy

Baseline SUV tertile	n	Mean baseline SUV and range	Slope ($\pm$SE)	Correlation coefficient (r)	Maximum detectable change in SUV* ($\pm$SE)
All	39	5.0 (1.6–12.3)	0.75 $\pm$ 0.08	0.84	81% $\pm$ 3%
First	13	2.5 (1.6–3.0)	0.40[†] $\pm$ 0.12	0.71	65%[‡] $\pm$ 5%
Second	13	4.2 (3.1–5.1)	0.98 $\pm$ 0.20	0.83	84% $\pm$ 7%
Third	13	8.2 (5.2–12.3)	0.83 $\pm$ 0.06	0.97[§]	90% $\pm$ 3%
Second and third	26	6.2 (3.1–12.3)	0.85 $\pm$ 0.10	0.89	86% $\pm$ 3%

*$| y$-intercept at $x = -100\%$ |.
[†]Value for first tertile was significantly different from that for other tertiles ($P \le 0.01$).
[‡]Value for first tertile was significantly different from that for other tertiles ($P \le 0.02$).
[§]95% confidence interval for third-tertile correlation coefficient (95% CI, 0.90–0.99) did not include first- and second-tertile correlation coefficients.

by dynamic nonlinear or graphic models and several static SUV algorithms.

We also investigated the range of maximum detectable percentage changes in SUV with therapy versus changes in MRFDG based on the range of pretherapy SUVs. We observed lower maximum detectable percentage changes in SUV associated with low pretherapy SUVs, as was expected and is likely due to a background of unmetabolized ^{18}F-FDG included in SUV measurements. This observation agrees with a recent breast cancer study that reported serial ^{18}F-FDG PET to be less accurate in response assessment for patients with low ^{18}F-FDG uptake on pretherapy scans (with a tumor-to-background ratio of less than 5) (22). A tumor-to-background ratio of 5 is comparable to an SUV of 2.5, assuming a typical normal breast tissue SUV of 0.5 (25), and agrees with our results for the patient tertile with the lowest baseline SUV average, 2.5. Both analyses suggest that caution should be taken when using percentage change in SUV to quantify response in patients with low pretherapy tracer uptake (SUV < 3). The dependence of the maximum detectable percentage change in SUV on pretherapy uptake illustrates the benefit of using dynamic kinetic analyses to measure response, especially for tumors with low ^{18}F-FDG uptake. We noted a small, statistically insignificant improvement in response classification for MRFDG versus SUV.

CONCLUSION

Chemotherapy and granulocyte CSF treatment resulted in a statistically significant lower amount of ^{18}F-FDG tracer in the blood AUC. The small decrease in mean concentration of ^{18}F-FDG in the blood did not have a large impact on the ability of changes in SUV to predict patient pathologic response to granulocyte CSF–containing chemotherapy regimens. The maximum detectable percentage change in ^{18}F-FDG uptake was lower when quantification was via static SUV versus dynamic MRFDG. This effect is small but may have clinical significance for measuring the response of patients with low pretherapy ^{18}F-FDG uptake (SUV < 3).

REFERENCES

1. Shankar LK, Hoffman JM, Bacharach S, et al. Consensus recommendations for the use of ^{18}F-FDG PET as an indicator of therapeutic response in patients in National Cancer Institute Trials. *J Nucl Med.* 2006;47:1059–1066.
2. Lammertsma AA, Hoekstra CJ, Giaccone G, Hoekstra OS. How should we analyse FDG PET studies for monitoring tumour response? *Eur J Nucl Med Mol Imaging.* 2006;33(suppl 13):16–21.
3. Weber WA, Wieder H. Monitoring chemotherapy and radiotherapy of solid tumors. *Eur J Nucl Med Mol Imaging.* 2006;33(suppl 13):27–37.
4. Keyes JW. SUV: standard uptake or silly useless value? *J Nucl Med.* 1995;36:1836–1839.
5. Huang SC. Anatomy of SUV: standardized uptake value. *Nucl Med Biol.* 2000;27:643–646.
6. Mankoff DA, Muzi M, Krohn KA. Quantitative positron emission tomography imaging to measure tumor response to therapy: what is the best method? *Mol Imaging Biol.* 2003;5:281–285.
7. Phelps M, Huang S, Hoffman E. Tomographic measurement of local cerebral glucose metabolic rate in humans with (^{18}F)2-fluoro-2-deoxy-D-glucose: validation of method. *Ann Neurol.* 1979;6:371–388.
8. Reivich M, Alavi A, Wolf A, et al. Glucose metabolic rate kinetic model parameter determination in humans: the lumped constant and rate constants for [^{18}F]fluorodeoxyglucose and [^{11}C]deoxyglucose. *J Cereb Blood Flow Metab.* 1985;5:179–192.
9. Gjedde A. Calculation of cerebral glucose phosphorylation from brain uptake of glucose analogs in vivo: a re-examination. *Brain Res.* 1982;4:237–274.
10. Patlak CS, Blasberg RG, Fenstermacher JD. Graphical evaluation of blood-to-brain transfer constants from multiple-time uptake data. *J Cereb Blood Flow Metab.* 1983;3:1–7.
11. Freedman NM, Sundaram SK, Kurdziel K, et al. Comparison of SUV and Patlak slope for monitoring of cancer therapy using serial PET scans. *Eur J Nucl Med Mol Imaging.* 2003;30:46–53.
12. Weber WA, Ziegler SI, Thodtmann R, Hanauske AR, Schwaiger M. Reproducibility of metabolic measurements in malignant tumors using FDG PET. *J Nucl Med.* 1999;40:1771–1777.
13. Graham MM, Peterson LM, Hayward RM. Comparison of simplified quantitative analyses of FDG uptake. *Nucl Med Biol.* 2000;27:647–655.

14. Sugawara Y, Zasadny KR, Kison PV, Baker LH, Wahl RL. Splenic fluoro-deoxyglucose uptake increased by granulocyte colony-stimulating factor therapy: PET imaging results. *J Nucl Med.* 1999;40:1456–1462.

15. Jacene HA, Ishimori T, Engles JM, Leboulleux S, Stearns V, Wahl RL. Effects of pegfilgrastim on normal biodistribution of ^{18}F-FDG: preclinical and clinical studies. *J Nucl Med.* 2006;47:950–956.

16. Krak NC, van der Hoeven JJ, Hoekstra OS, Twisk JW, van der Wall E, Lammertsma AA. Measuring [^{18}F]FDG uptake in breast cancer during chemotherapy: comparison of analytical methods. *Eur J Nucl Med Mol Imaging.* 2003;30:674–681.

17. Mankoff DA, Dunnwald LK, Gralow JR, et al. Blood flow and metabolism in locally advanced breast cancer: relationship to response to therapy. *J Nucl Med.* 2002;43:500–509.

18. Mankoff DA, Dunnwald LK, Gralow JR, et al. Changes in blood flow and metabolism in locally advanced breast cancer treated with neoadjuvant chemotherapy. *J Nucl Med.* 2003;44:1806–1814.

19. Tseng J, Dunnwald LK, Schubert EK, et al. ^{18}F-FDG kinetics in locally advanced breast cancer: correlation with tumor blood flow and changes in response to neoadjuvant chemotherapy. *J Nucl Med.* 2004;45:1829–1837.

20. Ellis GK, Livingston RB, Gralow JR, Green SJ, Thompson T. Dose-dense anthracycline-based chemotherapy for node-positive breast cancer. *J Clin Oncol.* 2002;20:3637–3643.

21. Kroep JR, Van Groeningen CJ, Cuesta MA, et al. Positron emission tomography using 2-deoxy-2-[^{18}F]-fluoro-D-glucose for response monitoring in locally advanced gastroesophageal cancer; a comparison of different analytical methods. *Mol Imaging Biol.* 2003;5:337–346.

22. McDermott GM, Welch A, Staff RT, et al. Monitoring primary breast cancer throughout chemotherapy using FDG-PET. *Breast Cancer Res Treat.* August 9, 2006 [Epub ahead of print].

23. DeLong ER, DeLong DM, Clarke-Pearson DL. Comparing the areas under two or more correlated receiver operating characteristic curves: a nonparametric approach. *Biometrics.* 1988;44:837–845.

24. Hoekstra CJ, Hoekstra OS, Stroobants SG, et al. Methods to monitor response to chemotherapy in non-small cell lung cancer with ^{18}F-FDG PET. *J Nucl Med.* 2002;43:1304–1309.

25. Zasadny KR, Wahl RL. Standardized uptake values of normal tissues at PET with 2-[fluorine-18]-fluoro-2-deoxy-D-glucose: variations with body weight and a method for correction. *Radiology.* 1993;189:847–850.